Journal of Cellular Biochemistry 104:418–434 (2008)

Calcium- and pH-Dependent Localization of Annexin A6 Isoforms in Balb/3T3 Fibroblasts Reflecting Their Potential Participation in Vesicular Transport

Agnieszka Strzelecka-Kiliszek,[1] Malgorzata E. Buszewska,[1] Paulina Podszywalow-Bartnicka,[1] Slawomir Pikula,[1] Katarzyna Otulak,[1] Rene Buchet,[2] and Joanna Bandorowicz-Pikula[1]*

[1]Department of Biochemistry, Nencki Institute of Experimental Biology, Warsaw, Poland
[2]Université de Lyon, Lyon, F-69603, France; Université Lyon 1, Villeurbanne, F-69622, France; INSA-Lyon, Villeurbanne, F-69622, France; CPE Lyon, Villeurbanne, F-69616, France; ICBMS, CNRS UMR 5246, Villeurbanne, F-69622, France

Abstract Annexin A6 (AnxA6), calcium- and membrane-binding protein, is involved in membrane dynamics. It exists in the cell in two isoforms, AnxA6-1 and AnxA6-2, varying only by the VAAEIL sequence. In most cells, AnxA6-1 predominates. A limited number of observations suggests that both isoforms differ from each other functionally. The EGF-dependent Ca^{2+} influx in A431 cells is inhibited only by AnxA6-1. Moreover, AnxA6-2 was found to exhibit higher affinity for Ca^{2+}. In this report we addressed the potential significance of the VAAEIL deletion in AnxA6-2. For this purpose, we expressed AnxA6 isoform cDNAs in bacteria or mouse Balb/3T3 fibroblasts. The recombinant AnxA6-2 was characterized by a less extended molecular shape than that of AnxA6-1 and required a narrower [Ca^{2+}] range to bind liposomes. Upon lowering pH in the presence of EGTA recombinant AnxA6-2 became less hydrophobic than AnxA6-1 as revealed by the Triton X-114 partition. Furthermore, AnxA6-2 revealed stronger F-actin binding than that of AnxA6-1. Immunofluorescence microscopy showed that the EGFP-tagged AnxA6 isoforms expressed in Balb/3T3 fibroblasts relocate in a Ca^{2+}- and H^+-sensitive manner to the vesicular structures in a perinuclear region or in cytosol. Cell fractionation showed that in resting conditions AnxA6-1 is associated with early endosomes and AnxA6-2 with late endosomes, and an increase in [Ca^{2+}] and/or [H^+] induced their opposite distribution. These findings suggest a potentially independent regulation, localization, and function of AnxA6 isoforms in Balb/3T3 fibroblasts. More generally, our findings suggest distinct functions of AnxA6 isoforms in membrane dynamics. J. Cell. Biochem. 104: 418–434, 2008.

Key words: annexin A6 isoforms; Balb/3T3 cells; endocytosis; cytoskeleton

Annexin A6 (AnxA6) is the largest member of the vertebrate family of ubiquitous calcium- and membrane-binding proteins with not yet clearly defined physiological functions. Experimental data obtained with reconstituted systems, cellular models, or transgenic animals, provided evidence of AnxA6 being involved in the cellular events such as regulation of membrane architecture [Draeger et al., 2005], calcium homeostasis and signaling [Song et al., 2002; Gerke et al., 2005], reorganization of cytoskeleton and vesicular traffic [Gerke and Moss, 2002; Rescher and Gerke, 2004; Rescher et al., 2004; Hayes et al., 2006], and signal transduction via Ras proteins [Davis et al., 1996; Pons et al., 2001]. Specifically, AnxA6, due to its involvement in the budding from plasma membrane of

Abbreviations used: AnxA, vertebrate annexin; CD, circular dichroism; EE, early endosomes; EGFP, enhanced green fluorescent protein; HM, heavy membranes; IPTG, isopropyl-β-D-thiogalactopyranoside; LE, late endosomes; LUVs, large unilammellar vesicles (liposomes); PI, propidium iodide; PIC, protease inhibitor cocktail; PM, plasma membrane; PNS, post-nuclear supernatant; RT, reverse transcription.

Grant sponsor: Ministry of Science and Higher Education (Poland); Grant number: N401 049 32-1143.

*Correspondence to: Dr. Joanna Bandorowicz-Pikula, Department of Biochemistry, Nencki Institute of Experimental Biology, Polish Academy of Sciences, 3 Pasteur Street, 02-093 Warsaw, Poland.
E-mail: j.bandorowicz-pikula@nencki.gov.pl

Received 17 July 2007; Accepted 5 October 2007
DOI 10.1002/jcb.21632

clathrin coated pits [Lin et al., 1992] and dissociation of clathrin from cytoskeleton [Kamal et al., 1998], has been implicated in clathrin-dependent convergence of early endosomes [Naslavsky et al., 2003] and in the trafficking of LDL particles from endosomes to the prelysosomal compartment [Grewal et al., 2000]. However, these observations are contradictory to those showing that endocytosis occurs normally in A431 cells lacking AnxA6 [Smythe et al., 1994].

It is well established that cellular activities of AnxA6 are attributed to several functional domains which may be distinct from each other: Ca^{2+}- and lipid-binding domains [Benz et al., 1996; Montaville et al., 2002], a cholesterol-sensitive domain responsible for a Ca^{2+}-independent translocation of AnxA6 to endosomes upon cholesterol loading [de Diego et al., 2002], a pH-sensitive domain participating in a voltage-dependent ion channel activity of AnxA6 [Golczak et al., 2001a,b], an F-actin-binding domain playing a role in AnxA6-mediated reorganization of cytoskeleton and cellular shape [Filipenko and Waisman, 2001], a S100A11-binding region playing a role in the formation of signaling complexes at the level of the sarcolemma [Chang et al., 2007], and a linker region with T356 being a potential site for phosphorylation of AnxA6 by Src family kinases and protein kinase C [Dubois et al., 1995; Schmitz-Peiffer et al., 1998; Freye-Minks et al., 2003]. The latter region is also involved in the interaction with $p120^{GAP}$ [Chow and Gawler, 1999; Grewal et al., 2005] and syndecan-2 [Huang et al., 2005]. In addition, a putative GTP-binding domain, a prerequisite for nucleotide-induced ion channel activity of AnxA6 at pH 7.0, has been identified [Kirilenko et al., 2006].

The understanding of AnxA6 functions is complicated by the fact that due to alternative mRNA splicing AnxA6 is expressed in mammalian tissues as two isoforms (longer AnxA6-1 and shorter AnxA6-2) varying by the 524-VAAEIL-529 sequence [Davies et al., 1989]. AnxA6-1 prevails in normal tissues [Kaetzel et al., 1994] and cells, such as mouse Balb/3T3 fibroblasts, while AnxA6-2 is more abundant in neoplastic cells [Edwards and Moss, 1995]. Any relationship between the level of expression of AnxA6 isoforms and neoplastic transformation is at present unknown. Concerning the functional differences between isoforms, the available data suggest that the EGF-dependent Ca^{2+} influx in A431 cells transfected with AnxA6 isoforms is specifically inhibited by AnxA6-1 and that the smaller splice variant has no discernible effect on cellular phenotype and growth rate [Fleet et al., 1999]. On the other hand, AnxA6-2 is characterized by a higher affinity for Ca^{2+}, lower hydrophobicity and lower negative surface charge, as compared to AnxA6-1 [Kaetzel et al., 1994].

By searching protein databases, we found proteins containing the VAAEIL sequence, including ADAM33 (Zn^{2+}-dependent metalloprotease), ABC-type metal ion transporters, ORF proteins, zinc finger NS5A protein, threonine dehydratase, glutamate dehydrogenase isozymes, and the small GTPase Rab28. The latter has been described to undergo alternative mRNA splicing near VAAEIL generating two isoforms, Rab28S and Rab28L, which differ in their tissue distribution; Rab28S being present in most of the investigated tissues, and Rab28L predominating in testis [Brauers et al., 1996]. By analogy, we reasoned that due to the presence or absence of VAAEIL AnxA6 isoforms may be differentially targeted to specific cellular compartments where they may elicit an isoform-specific regulatory function. In this work our intention was to verify the hypothesis that the different expression of AnxA6 isoforms in normal and pathological cells may reflect distinct regulation and localization of these isoforms in the cell.

Due to the difficulties in purifying AnxA6 isoforms from the cells or tissues, we produced the expression vector for AnxA6-2 using cDNA for AnxA6-1 as a template and created a deletion mutant lacking VAAEIL. Then, we expressed both isoforms in bacteria (to investigate physico-chemical propertes of the proteins) or in Balb/3T3 fibroblasts (to follow their intracellular localization). Our findings showed structural and functional differences between AnxA6 isoforms in cells. The properties of their Ca^{2+}- and pH-dependent translocation between early and late endosomes were different. We suggest that AnxA6 isoforms participate in membrane dynamics during vesicular transport.

MATERIALS AND METHODS

Expression of Human Annexin A6 Isoforms in *Escherichia coli* and Their Purification

Human AnxA6-2 cDNA was obtained by site-directed mutagenesis method using the cDNA

for AnxA6-1. The reaction mixture contained 125 ng (0.25 μl) of cDNA of AnxA6-1 as the matrix for PCR reaction, 125 ng (1 μl) of a primer for AnxA6-1 (5′-CCAggCAcgggAAgATgCCCAgg AAATAgCAgACACACCC-3′), 125 ng (1 μl) of a primer for AnxA6-2 (5′-gggTgTgTCTgCTATTT CCTgggCATCTTCCCgTgCCTgg-3′), and 0.5 mM (0.5 μl) each of four deoxynucleotide triphosphates in 25 μl of a PCR buffer [20 mM Tris–HCl, pH 8.8, 10 mM KCl, 10 mM $(NH_4)_2SO_4$, 2 mM $MgSO_4$, 1% Triton X-100, 1 mg/ml bovine serum albumin]. The mixture was denatured by heating at 95°C for 5 min and after cooling to 75°C 1 μl of Pfu Turbo polymerase was added. PCR amplification was carried out for 18 cycles using a step program. The cycles were as follows: denaturation for 2 min at 95°C, reannealing for 1 min at 55°C, and extension for 10 min at 68°C. The cycles were followed by a 5 min final extension period at 68°C. At the beginning, the onset of mutation from cDNA of AnxA6-1 occurred. Then, the synthesis of complementary plasmid DNA with breaks took place. At the end, 1 μl of DpnI was added and reaction was performed at 37°C for 90 min. Aliquots (10 μl) of the reaction mixture were then analyzed by 12% SDS–PAGE after staining with ethidium bromide. For purification of recombinant proteins, both isoforms were expressed in *Escherichia coli* after induction with isopropyl-β-D-thiogalactopyranoside (IPTG) and purified to homogeneity as described previously [Burger et al., 1993; Kirilenko et al., 2002] with small modifications.

Characterizations of Human Recombinant AnxA6 Isoforms

Gel electrophoresis. Ten microgram of human recombinant AnxA6 isoforms were analyzed in 5–12% polyacrylamide gels in 25 mM Tris–HCl, pH 8.8, 192 mM glycine without SDS. The gels were stained with Coomassie brilliant blue. The coefficients of retardation were obtained from logarithmic function of the migration (Log Rf) against concentrations of polyacrylamide [Rodbard and Chrambach, 1971].

CD spectra. Secondary structures of AnxA6 isoforms in 5 mM Tris–HCl, pH 7.4, 20 mM NaCl, 1 mM EGTA at room temperature were calculated from CD spectra (AVIV Associates Incorporation) using CDSSTR software [Golczak et al., 2001a,b].

F-actin binding. Rabbit skeletal muscle F-actin binding of human recombinant AnxA6 isoforms (1:1 molar ratio) were tested by a pelleting assay [Dominik et al., 2005]. The assay mixture was centrifuged at 200,000*g* for 60 min, followed by the determination of densitometry of the gels using Ingenius software (BioRad).

Binding to liposomes. Large unilammellar liposomes (LUVs) were prepared from asolectin in the presence of 250 mM sucrose [Reeves and Dowben, 1969]. To examine the binding of human recombinant AnxA6 isoforms to liposomes, 10 μg of human recombinant AnxA6 isoforms were incubated for 1 h at room temperature with 5 μg of LUVs in: (i) 10 mM Tris–HCl buffer, pH 7.5, 50 mM NaCl, 1 mM EGTA, 250 mM sucrose, and from 2×10^{-10} to 4×10^{-3} M Ca^{2+} (calculated using Chelator software) or (ii) either 10 mM citric (pH 3.6–6.5) or 10 mM Tris–HCl (pH 7.0–8.0) buffer, 50 mM NaCl, 1 mM EGTA, 250 mM sucrose. Liposomes were then centrifuged at 12,000*g*/10 min, supernatants were collected and protein concentration was determined [Bradford, 1976]. Pellets were washed in 10 mM Tris–HCl, pH 7.5 supplemented with 2 mM $CaCl_2$ (for Ca^{2+}-dependent binding) or in buffers of appropriate pH values (for H^+-dependent binding), centrifuged as above, and subjected to 12% SDS–PAGE followed by Coomassie brilliant blue staining. The binding of AnxA6 isoforms to LUVs was estimated by densitometric analysis of the gels.

Phase separation in Triton X-114. The temperature-induced phase separation test was performed as described by Bordier [1981] with modifications according to Hooper [1992]. Human recombinant AnxA6 isoforms (0.2 mg/ml) were incubated in 200 μl buffer containing 10 mM Tris–HCl, pH 7.4, 6.0, 5.0, or 4.0, 150 mM NaCl, 5 mM EGTA, or 1 mM $CaCl_2$ and 0.5% (w/v) Triton X-114 for 15 min at 4°C. Then it was layered on 300 μl 10 mM Tris–HCl, pH 7.4, 6.0, 5.0, or 4.0, 150 mM NaCl, 5 mM EGTA, or 1 mM $CaCl_2$, 6% (w/v) sucrose, and 0.06% (w/v) Triton X-114, and incubated for 10 min at 30°C. It was centrifuged for 10 min at 1,000*g* at room temperature. The upper aqueous phases were collected and treated with fresh 0.5% (w/v) Triton X-114 solution for 5 min at 4°C, loaded onto a sucrose cushion, incubated for 5 min at 30°C and centrifuged as described above. The upper aqueous phases were collected, while the intermediate sucrose phases were

removed to collect bottom final detergent phases. Aqueous phases were additionally treated with fresh 2% (w/v) Triton X-114 solution for 5 min at 4°C, incubated for 5 min at 30°C and centrifuged as described above. Supernatants (200 μl) were collected as final aqueous phases. Aliquots of the separated phases were subjected to SDS–PAGE and the amount of proteins was determined by densitometric analysis of the gel.

Cell Cultures and Cell Stimulation With Extracellular Ca^{2+} or H^{+}

Mouse Balb/3T3 embryo fibroblasts (ATCC CCL-163) were cultured in DMEM supplemented with 100 U/ml penicillin, 100 μg/ml streptomycin, 2 mM L-glutamine (all from Sigma) and 10% FBS (Gibco). Cells were stimulated for 10 min at room temperature by incubating in the PD buffer (125 mM NaCl, 5 mM KCl, 10 mM $NaHCO_3$, 1 mM KH_2PO_4, 10 mM glucose, 1 mM $MgCl_2$, 20 mM Hepes, pH 6.9) [Strzelecka et al., 1997] supplemented with 1 mM $CaCl_2$ or 5 mM EGTA, and adjusted to pH 7.4 or 6.0. Time-dependent changes in intracellular $[Ca^{2+}]$ or pH in Balb/3T3 cells were measured by means of a Shimadzu RF5000 fluorimeter, using Fura-2/AM and BCECF/AM (both from Molecular Probes), respectively [Zablocki et al., 2003]. Briefly, Balb/3T3 cells (5×10^6) were loaded with 1 μM of Fura-2/AM or BCECF/AM by incubation in 5 ml of the culture medium at 37°C for 15 min. Then, the cells were washed and suspended in 3 ml of the PD buffer (pH 7.4 or 6.0) supplemented with 1 mM $CaCl_2$ (called throughout stimulating medium). Intracellular $[Ca^{2+}]$ was calibrated in each run using 3 mM external $CaCl_2$ plus 3 μM ionomycin (Sigma) followed by 3 μM digitonin (Sigma) and 100 mM EGTA, whereas calibration of pH was performed by titration with NaOH or HCl in the presence of 3 μM digitonin.

Characterizations of Mouse Balb/3T3 Embryo Fibroblasts

Determination of messenger RNA for Annexin A6 in Balb/3T3 cells by reverse transcription PCR. Three hundred twenty microgram of total RNA was isolated from 10^7 Balb/3T3 cells using Trizol (Invitrogen). 50 pmol (1 μl) of right primer (T_m 73°C) was added and 10 μg of total RNA (1 μl) were annealed at 70°C for 5 min, then cooled on ice. The reverse transcription (RT) reaction was initiated by adding 1 mM (1 μl) of dNTP, 40 U (1 μl) RNAse inhibitor (Roche), 80 U (2 μl) of M-MuLV reverse transcriptase (Roche) in a total volume of 25 μl of cDNA synthesis buffer (50 mM Tris–HCl, 40 mM KCl, 6 mM $MgCl_2$, 10 mM DTT, pH 8.3, Roche). cDNA was analyzed by polymerase chain reaction (PCR) using primer pairs specific for either AnxA6 (matrix AnxA6-1 mouse complete cDNA NM_013472, accession number—1593-1730) and GAPDH as control (matrix GAPDH mouse complete cDNA M 32599, accession number—382-916). Primer pairs generated a 137 bp cDNA fragment of AnxA6-1 (the VAAEIL insert), a 119 bp cDNA fragment of AnxA6-2 (the VAAEIL deletion), and a 538 bp cDNA fragment of GAPDH. The reaction mixture was incubated at 37°C for 60 min. The enzyme was inactivated at 95°C for 3 min. The reaction was repeated with a newly added enzyme. The RT reaction mixtures were subjected to PCR amplification by adding 500 pmol (0.25 μl) of the right and left primers each and 1 U of Taq DNA polymerase (Invitrogen) in a total volume of 50 μl of PCR buffer (20 mM Tris–HCl, pH 8.4, 50 mM KCl, 1.5 mM $MgCl_2$, Invitrogen). The mixture was denatured by heating at 95°C for 5 min and after cooling to 75°C the enzyme was added. PCR amplification was carried out for 35 cycles using a step program. Aliquots (10 μl for AnxA6 and 4 μl for GAPDH) of the reaction were then analyzed by 12% SDS–PAGE with RNA ethidium bromide staining and semi-quantified (Ingenius software, BioRad).

Expression of human Annexin A6 isoforms in mouse Balb/3T3 fibroblasts. To express AnxA6 isoforms in Balb/3T3 fibroblasts cDNAs encoding human AnxA6 isoforms [tagged with enhanced green fluorescent protein (EGFP) at 3′-end of the cDNA] were subcloned into the eukaryotic expression vector pEGFP-N3 (BD Biosciences Clontech). Then, Balb/3T3 cell suspension (10^5 cells/ml) was stably transfected with the empty pEGFP-N3 vector or the fusion constructs (EGFP-AnxA6-1 or EGFP-AnxA6-2) using the effectene transfection reagent (Qiagen GmbH), in the cDNA: effectene ratio of 1:20. After 48 h incubation 1 mg/ml G418 (Sigma) was added to the culture medium for 7 days. To isolate clones overexpressing AnxA6 or its splice variant, G418-resistant cells were cultured with 0.5 mg/ml G418. After 30 days selection, AnxA6 isoforms expressing cells were tested by FACScan

and Western blot methods. As a control non-transfected cells cultured without G418 were used.

FACScan analysis. The number of cells expressing empty pEGFP-N3 vector or the fusion constructs (pEGFP-AnxA6-1 or pEGFP-AnxA6-2) was counted by means of FACScan flow cytometer (Becton-Dickinson) using Cell Quest software (Becton-Dickinson) from 10^4 cells for each experimental set. To identify viable cells [Krishan, 1975], transfected or non-transfected cells (10^6) were washed twice with the PD buffer, then suspended in 2 ml 50 μg/ml propidium iodide (PI) in PD, incubated for 5 min at room temperature and used directly for flow analysis of PI fluorescence. For cell cycle analysis [Dressler, 1988], cells (3×10^6) were centrifuged at 2,500*g*/5 min and the pellet was suspended in 1 ml PBS. Cell suspension was added into absolute 70% (v/v) EtOH final concentration and fixed overnight at −20°C. Then cells were centrifuged, suspended in 50 μg/ml PI in PBS containing 0.1 mg/ml RNAse and 0.05% Triton X-100, incubated for 40 min at 37°C, centrifuged, suspended in 2 ml PBS and analyzed for flow PI fluorescence. In both PI staining methods FL2 (470 V linear) emission channel was used to monitor PI fluorescence, where the size [forward scatter of cells (FSC), 100–400 of FSC-Height] and the granularity [side scatter of cells (SSC), 200–600 of SSC-Height] of the cells were analyzed. The absolute numbers of all cells were determined from light scatter FSC/SSC, double discrimination of the fluorescence peak integral and height, and EGFP fluorescence intensity (to measure the transfection efficiency) [Kim et al., 2007].

Immunocytochemistry. Balb/3T3 cell suspension was applied onto acid-washed glass cover-slips placed in Petri dishes and cultured 20 h at 37°C in 5% CO_2 humidified atmosphere. Cells (10^5) in resting or stimulated buffers were fixed with 3% paraformaldehyde/PD for 20 min at room temperature (rt) [Strzelecka et al., 1997]. The fixed transfected cells were washed twice with PD and once with H_2O and mounted in Moviol 4-88 (Calbiochem) supplemented with 2.5% DABCO (Sigma). The fixed non-transfected cells were washed with the PD buffer, incubated in 50 mM NH_4Cl/PD (10 min, rt) and after washing permeabilized with 0.08% Triton X-100/PD (5 min, 4°C). After additional washing once with PD and then once with TBS (130 mM NaCl, 25 mM Tris–HCl, pH 7.5), the cells were incubated with blocking solution (5% FBS/TBS) for 45 min at rt. The cells were incubated for 1 h at rt with different primary antibodies: mouse monoclonal anti-AnxA6 (1:200) (Transduction Laboratories), rabbit polyclonal anti-AnxA6 (1:100), rabbit polyclonal anti-Rab5B (1:100), rabbit polyclonal anti-Rab7 (1:100), or mouse monoclonal anti-SNAP-25 (1:100) (all Santa Cruz Biotechnology). Then, they were washed (6×5 min) with 0.5% FBS/TBS/0.05% Tween20 and incubated for 1 h at rt with appropriate secondary antibody: goat anti-mouse IgG-FITC (1:500), goat anti-mouse IgG-rhodamine (1:500), or goat anti-rabbit IgG-TRITC (1:500) (all Sigma). All antibodies were prepared in 0.5% FBS/TBS/0.05% Tween20. After washing (four times in 0.5% FBS/TBS/0.05% Tween20, two times in TBS and one time in H_2O) the samples were mounted in Moviol 4-88/DABCO. Z-section images were acquired with TCS SP2 confocal microscope (Leica).

Cell membrane fractionation. For Ca^{2+}, EGTA extraction of membranes the transfected or non-transfected Balb/3T3 cells (10^8) were washed twice with PD, solubilized as described by Babiychuk and Draeger [2006] with modifications in a Triton lysis buffer (TLB) containing 0.05% Triton X-100, 50 mM Tris–HCl, pH 7.4, 80 mM NaCl, 10 μg/ml protease inhibitor cocktail (PIC, Sigma) [Strzelecka-Kiliszek et al., 2002] with 2 mM $CaCl_2$ (TLBA) or 5 mM EGTA (TLBB). Cells were homogenized by 20 passes through a 22-gauge syringe needle and disrupted by repeated sonication cycles (Branson ultrasonic Sonifier S-250D). After lysis (30 min/4°C) cells were centrifuged (100,000*g*/15 min/4°C) in Sorval AH-4 rotor [Clemen et al., 1999]. Supernatants (S1) were collected whereas pellets (P1) were suspended in TLB with 20 mM EGTA (TLBC). After incubation (30 min/4°C) samples were centrifuged as above. Supernatants (S2) were collected whereas pellets (P2) were suspended in TLBC. SDS–PAGE loading buffer (SPLB) contained 2% SDS, 10% glycerol, 250 mM Tris–HCl, pH 6.8, 1.25 mg/ml bromophenol blue, and 1% β-mercaptoethanol. Then probes were boiled for 5 min and stored at −20°C. For examination of subcellular distribution of AnxA6 transfected or non-transfected Balb/3T3 cells (1.5×10^8) were subjected for sucrose density gradient fractionation [Grewal et al., 2000]. Cells were washed twice with the PD buffer. After stimulation cells were put on

ice, washed with cold 0.5% FBS/PBS and collected in homogenization buffer (HB, 250 mM sucrose, 3 mM imidazole, pH 7.4, and 10 μg/ml PIC). Then, cells were pelleted, suspended in 1 ml of HB and homogenized by 50 passages through a 22-gauge syringe needle. The homogenate was centrifuged 1,200*g*/15 min/4°C in an Eppendorf centrifuge. The post-nuclear supernatant (PNS) was brought to a final 40.2% sucrose (w/v) concentration by adding 62% sucrose/3 mM imidazole, pH 7.4 and loaded at the bottom of a 5 ml centrifugation tube (Kendro Laboratory Products). Then, 35% sucrose, 25% sucrose, and finally HB were poured stepwise on top of the PNS. The gradient was centrifuged at 220,000*g*/120 min/4°C in Sorval AH-650 rotor. After centrifugation, three interphases: 1 (8%/25% or 1.09 g/cm^3), 2 (25%/35% or 1.115 g/cm^3), and 3 (35%/40.2% or 1.12–1.2 g/cm^3) were collected starting from the top, mixed with SPLB, boiled for 5 min and stored at −20°C. The protein concentration was determined [Bradford, 1976]. The presence of AnxA6 and markers, Rab5B (of early endosomes, EE), Rab7 (of late endosomes, LE), and SNAP-25 (of plasma membrane, PM), were checked by Western blotting. The distribution of AnxA6 isoforms in the interphases was quantified using Ingenius software (BioRad).

Western blotting. Proteins were separated on 10% SDS–PAGE and transferred onto nitrocellulose sheets. Immunoblots were washed with TBS and then incubated 1 h at rt in blocking solution (5% non-fat milk/TBS). After washing with TBS containing 0.05% Tween20 (TBST), they were probed overnight at 4°C with primary antibodies—mouse monoclonal anti-AnxA6 (1:2,500), mouse monoclonal anti-AnxA2 (1:2,500) (both from Transduction Laboratories), rabbit polyclonal anti-Rab5B (1:200), rabbit polyclonal anti-Rab7 (1:200), and mouse monoclonal anti-SNAP-25 (1:200) (all from Santa Cruz Biotechnology). After washing with TBST the blots were treated for 1.5 h at rt with appropriate secondary antibodies—sheep anti-mouse or donkey anti-rabbit IgG-horseradish peroxidase conjugates (1:5,000) (Amersham Biosciences). All antibodies were prepared in 5% non-fat milk/TBST. To analyze other antigens on the same nitrocellulose sheets bound antibodies were removed by incubation in stripping buffer (100 mM β-mercaptoethanol, 2% SDS, 62.5 mM Tris–HCl, pH 6.7, 30 min/50°C), washed and then incubated 1 h at rt in blocking solution. As reported above, the whole procedure of washing, incubation with primary antibody rabbit anti-GFP (N-ter) (1:1,000) (Sigma), washing and treatment with secondary antibody—donkey anti-rabbit IgG-horseradish peroxidase conjugate were performed under the same conditions. After washing (several changes of TBST and then once with TBS) immunoreactive bands were visualized using ECL reagents (Amersham Biosciences).

RESULTS

Biochemical Characterization of Recombinant Human Annexin A6 Isoforms

To investigate the properties of AnxA6 isoforms in vitro and ex vivo, we generated a deletion mutant of AnxA6-1 lacking the VAAEIL sequence, therefore mimicking AnxA6-2, and used cDNAs encoding both isoforms to perform their heterologous expression in bacteria and in Balb/3T3 cells.

To gain information about the overall shape of the AnxA6 isoforms, the electrophoretic mobility of recombinant proteins purified from *E. coli* was examined in gels of polyacrylamide concentration varying from 5% to 12% under non-denaturing conditions. We observed that AnxA6-2 migrated substantially slower than AnxA6-1 in 5–7% polyacrylamide, probably due to the absence of the negatively charged residue E528, but slightly faster in 12% polyacrylamide, suggesting a less extended shape in comparison to AnxA6-1 (Fig. 1A), as confirmed by analyzing the results of a Ferguson plot (Fig. 1B). Based on

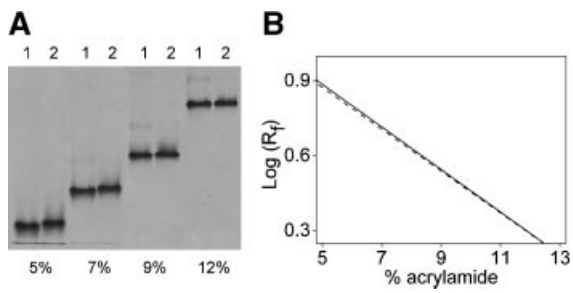

Fig. 1. Electrophoretical mobility of AnxA6-1 (**lanes 1**) and AnxA6-2 (**lanes 2**) under non-denaturing conditions. **A**: Each pair of lanes represents a single gel run at the indicated polyacrylamide concentration. To each gel lane 10 μg of protein were applied. The gels were stained with Coomassie brilliant blue. **B**: Ferguson plot of the migration of each isoform at different polyacrylamide concentrations. The data shown are typical of the results from three experiments; AnxA6-1, solid line; AnxA6-2, dashed line.

the interpretation given by Freye-Minks et al. [2003] who used same experiment to analyze properties of wild-type AnxA6 and its T356D mutant mimicking phosphorylation, the non-parallel slopes of linear fitting curves suggest different molecular shapes for the isoforms as evidenced by a higher retardation coefficient of AnxA6-1. These findings point to the existence of only subtle structural differences between the AnxA6 isoforms that are otherwise similar to each other with respect to their isoelectric pH and overall secondary structures derived from the CD spectra of both proteins (Table I).

Both recombinant AnxA6 isoforms purified from bacteria exhibited different actin-binding properties as determined by the actin-pelleting assay (Fig. 2), suggesting their potentially distinct participation in regulation of cytoskeleton dynamics in vivo. In the absence of F-actin, both isoforms were found, as expected, in the supernatants. In the presence of F-actin, AnxA6-1 was equally distributed between supernatant and pellet, whereas in the case of AnxA6-2 77% was bound to actin filaments.

Both recombinant AnxA6 isoforms were indistinguishable in vitro with respect to the calcium concentration required to exert half maximal binding to asolectin liposomes; $K_{1/2}$ amounted to 0.95×10^{-6} M and to 0.83×10^{-6} M for AnxA6-1 and AnxA6-2, respectively (Fig. 3A). However, the sensitivity of AnxA6-2 for Ca^{2+} was characterized by a narrower concentration range than for AnxA6-1 (2.37×10^{-7}–3.27×10^{-6} M for AnxA6-2 compared to 4.04×10^{-8}–4.79×10^{-5} M for AnxA6-1). Furthermore, half-maximal binding of both isoforms to asolectin liposomes occurred at pH 4.6–5.0 (Fig. 3B); however, AnxA6-2 responded over a broader pH range than AnxA6-1. This suggests varying ability of the isoforms to respond to changes of intracellular calcium and proton concentrations upon cell stimulation.

AnxA6 isoforms expressed and purified in *E. coli* were differently distributed in a [Ca^{2+}]- and pH-dependent manner into the detergent (hydrophobic) phase mimicking lipid bilayer

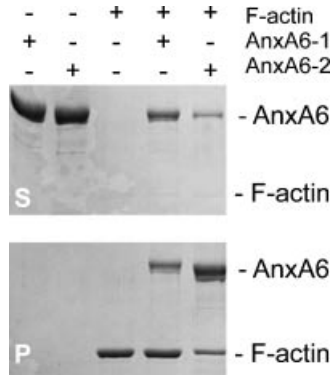

Fig. 2. Binding of AnxA6-1 and AnxA6-2 to F-actin. AnxA6 isoforms were incubated with F-actin at the 1:1 molar ratio and centrifuged as described in the Materials and Methods Section. For control AnxA6 isoforms or F-actin were incubated separately. The protein pattern in both supernatants and pellets was analyzed by SDS–PAGE followed by Coomassie brilliant blue staining. The positions of AnxA6 isoforms and F-actin are indicated. The result of one typical experiment out of three is shown; **S**, supernatant; **P**, pellet.

(Fig. 4). In the presence of EGTA, incubation of AnxA6-1 at pH 5.0 rendered the protein more hydrophobic than AnxA6-2 (Table II). At pH 4.0 the situation was opposite. In the presence of Ca^{2+} both isoforms were disappearing from aqueous phase in a similar manner, suggesting their common ability to undergo changes in hydrophobicity and conformation upon acidification [Golczak et al., 2001b].

Cellular Distribution of Annexin A6 Isoforms Is Regulated by Ca^{2+} and H^+

It is known that the longer variant AnxA6 predominates over AnxA6-2 in normal cells and tissues at a ratio of at least 3:1 [Kaetzel et al., 1994]. In order to determine the relative mRNA expression ratio in Balb/3T3 cells using RT-PCR, PCR primers were designed to span the splicing region of reverse transcribed RNAs (see the Materials and Methods Section). RT-PCR amplification of total cell RNA showed two bands corresponding to the predicted lengths of 119 and 137 bp for AnxA6-1 and AnxA6-2,

TABLE I. Characteristics of Human AnxA6 Isoforms

Isoform	pI[a]	α-Helices (%)	β-Structures (%)	Unordered (%)
AnxA6-1	5.51	70.3 ± 4.3	16.4 ± 0.8	13.3 ± 0.6
AnxA6-2	5.56	70.2 ± 3.8	16.9 ± 0.9	12.9 ± 0.6

[a]The isoelectric point. The secondary structure of the isoforms was computed using CDSSTR software on the basis of the CD spectra of AnxA6 recorded in the absence of calcium.

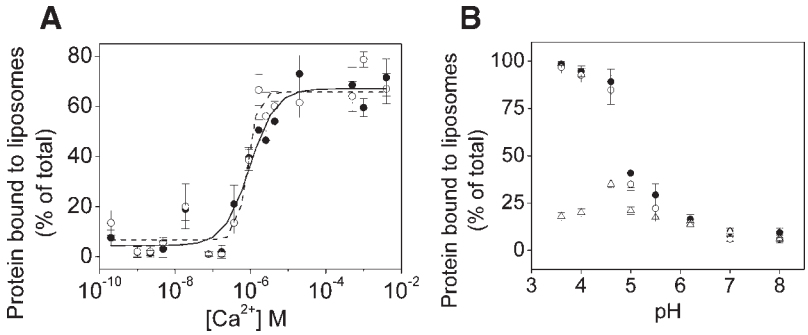

Fig. 3. Binding curves of AnxA6-1 (●) and AnxA6-2 (○) to asolectin liposomes as a function of [Ca^{2+}] (**A**) or [H^+] (**B**). AnxA6 isoforms bound to large unilammellar liposomes (LUVs) at indicated [Ca^{2+}] or pH values were separated from unbound proteins by centrifugation. Proteins in the pellet were analyzed by SDS–PAGE followed by Coomassie brilliant blue staining. Then, the amount of protein bound to LUVs proteins (expressed as % of total protein added) was determined by densitometric analysis and half-maximal binding of AnxA6-1 and AnxA6-2 to LUVs was calculated. Samples of AnxA6 isoforms incubated without liposomes served as a control (△). The mean of three independent experiments is shown.

respectively (Fig. 5). Their identity was confirmed by sequencing the gel purified bands. The ratio of AnxA6-1/AnxA6-2 in Balb/3T3 cells amounted to 4.6 ± 0.5.

To follow potential relocation of AnxA6 isoforms in the stimulated cells, we first analyzed the effects induced by elevated concentrations of Ca^{2+} and H^+ in external media on intracellular [Ca^{2+}] or pH in Fura-2 or BCECF loaded Balb/3T3 cells. By raising extracellular H^+ concentration from pH 7.4 to pH 6.0, in the presence of 1 mM $CaCl_2$, we observed some increase of intracellular [Ca^{2+}] from 145.5 ± 14.5 nM at pH 7.4 to 183.6 ± 17.4 nM at pH 6.0 after 200 s, whereas intracellular pH decreased from 6.91 ± 0.09 to 6.39 ± 0.12.

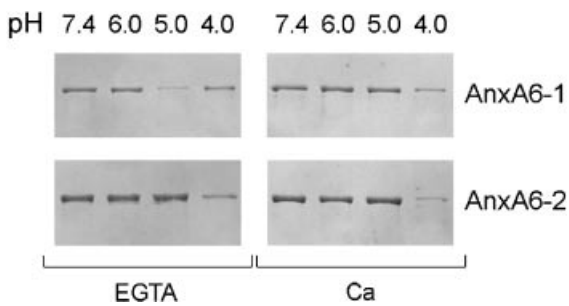

Fig. 4. Phase separation of AnxA6-1 and AnxA6-2 in Triton X-114 as a function of [Ca^{2+}] and [H^+]. The temperature-induced phase separation test was performed with 5 mM EGTA or 1 mM $CaCl_2$ at indicated pH values as described in Materials and Methods Section. Aliquots of the separated phases were analyzed by SDS–PAGE followed by Coomassie brilliant blue staining. The positions of AnxA6 isoforms are indicated. Protein composition of aqueous phases from a typical experiment is shown.

In parallel, by using the propidium iodide staining we examined whether or not the different extracellular environment with respect to pCa and pH affects cell survival and as a result, the localization of AnxA6. We first ensured that our experimental conditions had no significant effects on the cell viability (Fig. 6A), cell size (Fig. 6B), and cell granularity (Fig. 6C), and that there was no discernible effect on cell cycle, and only a minimal number of cells became apoptotic (Fig. 6D). Almost 50% of experimental as well as control cells were at G0 or G1 phase (Fig. 6E). Less then 20% of cells performed DNA synthesis and chromosome duplication (Fig. 6F). Up to 30% of cells were in G2 phase or performed chromosome separation, mitosis, and cell division (Fig. 6G). These results suggested that our experimental conditions did not stimulate cell apoptosis or cell proliferation. Then we examined whether or not the expression of AnxA6 isoforms affected cell survival (Fig. 7). Overexpression of AnxA6-2 isoforms affected cell viability up to 50% compared to the AnxA6-1 transfectants (80%). Non-transfected or transfected cells with empty plasmid exhibited the same level of cell survival (80%) (Fig. 7A). Overexpression of AnxA6-1 caused the decrease in the number of cells with regular size in comparison to control cells or cells overexpressing AnxA6-2 (Fig. 7B). The low number of cells with regular size (15%) in empty plasmid transfectants may be a natural reaction of cells in which EGFP protein persists in the nucleus [Wei et al., 2003]. Any type of transfection had a significant effect on the cell granularity (Fig. 7C).

TABLE II. Partition of AnxA6 Isoforms Into an Aqueous Phase in the Presence of Triton X-114

	+ EGTA				+ Ca^{2+}			
pH	4.0	5.0	6.0	7.4	4.0	5.0	6.0	7.4
AnxA6-1	8.9–11.4	1.9–2.2	10.3–13.5	11.0–15.1	6.2–7.2	16.2–16.4	14.5–17.1	14.9–17.9
AnxA6-2	4.9–6.0	15.7–18.1	17.1–17.2	17.9–18.1	2.0–4.7	14.0–20.6	12.7–18.0	14.8–22.3

The amount of protein in the aqueous phase is expressed as % of total protein used and was determined by densitometric analysis of the gels from two experiments.

Due to unavailability of antibodies specifically recognizing AnxA6 isoforms, we examined the distribution of endogenous AnxA6 in Balb/3T3 cells by immunocytochemistry. In control cells, after 10 min of incubation at pH 6.9, the main pool of endogenous AnxA6 was observed in cytosol, with only scattered staining at plasma membrane (data not shown). Previous studies have demonstrated a Ca^{2+}-dependent binding of AnxA6 to phospholipids in vitro [Bandorowicz et al., 1992]. To evaluate the effects of changes in intracellular [Ca^{2+}] and [H^+] on the distribution of endogenous AnxA6 in the cell, $[Ca^{2+}]_{in}$ and $[H^+]_{in}$ were manipulated by complementing the extracellular milieu with either 5 mM EGTA or 1 mM $CaCl_2$ and by varying extracellular pH. In the presence of 5 mM EGTA at pH 7.4, endogenous AnxA6 was uniformly distributed in the cell (Fig. 8A). The extracellular addition of 1 mM $CaCl_2$ at pH 6.0 resulted in the appearance of a punctate distribution of endogenous AnxA6 in cytosol (probably attached to endosomes) and on plasma membrane (Fig. 8D).

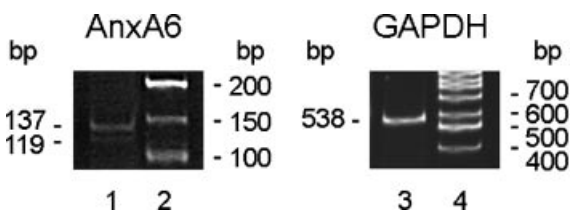

Fig. 5. Expression of endogenous AnxA6 isoforms in Balb/3T3 cells as analyzed by RT-PCR. Detection of RNA of AnxA6 isoforms (**lanes 1**, **2**) and GAPDH (**lanes 3**, **4**) using RT-PCR. 10^7 cells produced approximately 320 μg of total RNA and 10 μg of it were primed with an anti-sense primer, reverse transcribed with M-MuLV reverse transcriptase and further amplified by 35 PCR cycles. RT-PCR products (10 μl for AnxA6 and 4 μl for GAPDH) from Balb/3T3 cells (**lanes 1**, **3**) and oligonucleotide size standards (**lanes 2**, **4**) were separated in 12% SDS–PAGE and stained with ethidium bromide. The positions of the two amplification products of 119 and 137 bp and oligonucleotide size standards are indicated. The identity of the amplification products (see the Materials and Methods Section) as AnxA6 isoforms was confirmed by sequencing the gel purified bands.

As a next step, to dissect specific roles, if any, we expressed human AnxA6 isoforms in mouse Balb/3T3 cells. At pH 7.4 and in the presence of extracellular EGTA, AnxA6 isoforms displayed different cellular localizations in the stably transfected cells. AnxA6-1 existed in a vesicle-bound form in the perinuclear region of the cell (Fig. 8B) whereas AnxA6-2 was present in the vesicle-bound form in the cytosol (Fig. 8C). This was clearly different from the distribution of the fluorescent tag itself observed in control cells transfected with empty pEGFP-N3 vector (data not shown). The addition of 1 mM $CaCl_2$ at pH 6.0 resulted in AnxA6-1 relocation mainly to the plasma membrane (Fig. 8E) whereas Anx A6-2, similar to endogenous AnxA6, was distributed in cytosol (probably attached to endosomes) and on plasma membrane (Fig. 8F). These findings are consistent with a different sensitivity of recombinant isoforms to Ca^{2+} or H^+. Changes in the Ca^{2+} and H^+ concentrations had no effect on control cells transfected with empty pEGFP-N3 plasmid (data not shown).

Annexin A6 Isoforms Differ by Their Distribution Along the Endocytotic Pathway

To delineate the intracellular distribution of AnxA6 isoforms, we determined the expression of these isoforms at the protein level in transfected Balb/3T3 fibroblasts. Figure 9 shows a representative Western blot demonstrating the presence of exogenous AnxA6 isoforms in Balb/3T3 cells as compared with endogenous AnxA6 levels in the same cells, as well as non-transfected or empty pEGFP-N3 vector-transfected controls. The expression of AnxA6 isoforms in the cells did not result in a decreased level of endogenous AnxA6. To further analyze the intracellular distribution of AnxA6 isoforms, we fractionated cells into cytosolic and membrane fractions. Using different solubilization conditions, we observed that AnxA6 isoforms displayed different extractability by 0.05%

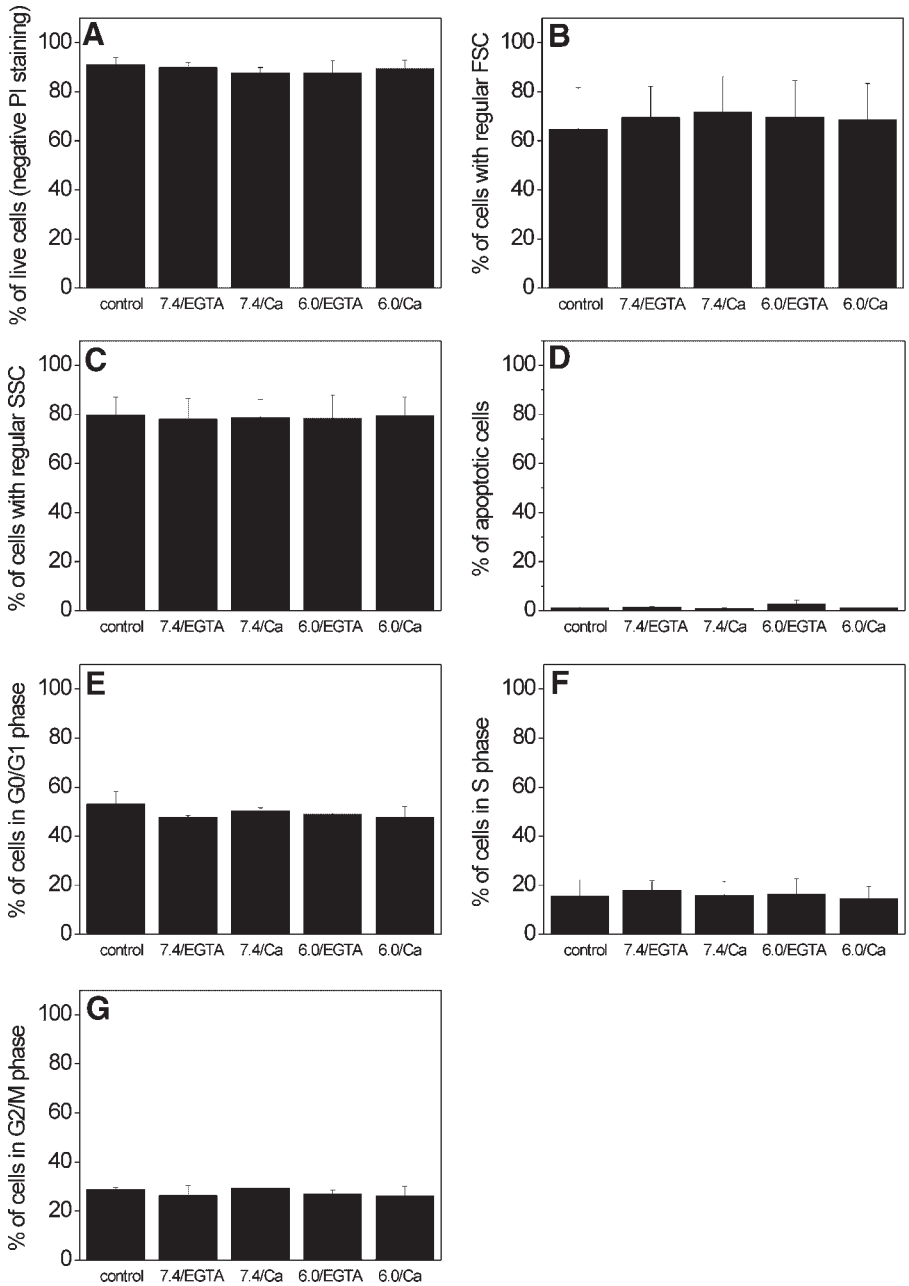

Fig. 6. The effect of changes in intracellular [Ca^{2+}] and [H^+] of Balb/3T3 cells induced by external pCa and pH on cellular viability, size, granularity, and cell cycle. Each panel (**A**–**G**) was labeled accordingly: untreated cells (control, **lane 1**) or incubated 10 min/20°C in different extracellular Ca^{2+} and H^+ concentrations in the PD buffer: pH 7.4/5 mM EGTA (**lane 2**), pH 7.4/1 mM $CaCl_2$ (**lane 3**), pH 6.0/5 mM EGTA (**lane 4**), or pH 6.0/ 1 mM $CaCl_2$ (**lane 5**). To identify live cells (**A**–**C**), 10^6 cells were washed, stained by PI and analyzed directly by means of flow cytometer to determine cell viability (**A**), cell size (**B**), and cell granularity (**C**). For cell cycle analysis (**D**–**G**) 3×10^6 cells were fixed, stained by PI, centrifuged, suspended in PBS and used for flow analysis of the apoptotic cells (**D**), the resting cells (**E**), DNA synthesis (**F**), and the cell division (**G**). The mean of two independent experiments is shown.

Triton X-100. Cell solubilization in the presence of 5 mM EGTA induced a release of both isoforms into cytosol, but a small pool still persisted in the membrane fraction. Under the same conditions, most of the endogenous AnxA6 remained in the membrane fraction and treatment with 20 mM EGTA was necessary to fully solubilize it. Densitometric analysis of the blot shown in Figure 9 revealed the occurrence of 23% of AnxA6-1 and 13% of AnxA6-2 in membrane fraction in the presence of 5 mM EGTA in the lysis buffer; under the same

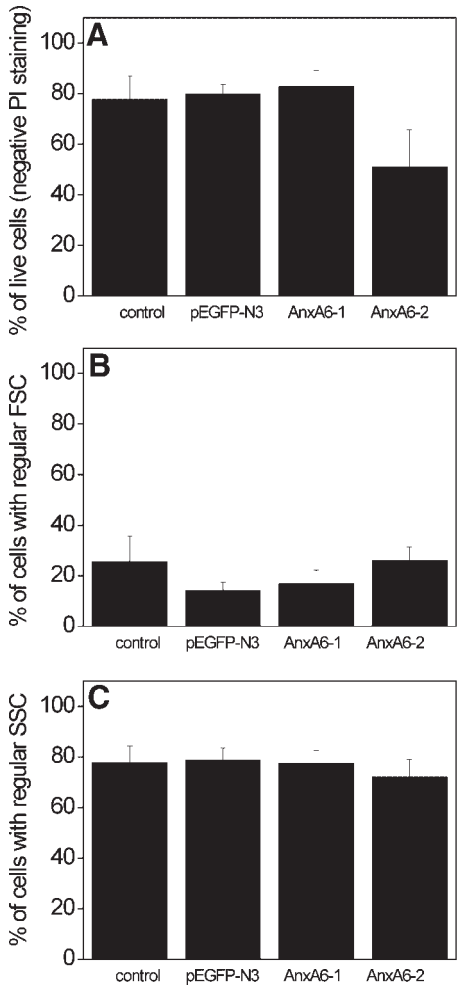

Fig. 7. The effect of AnxA6 isoforms expression on cellular viability, size, and granularity of transfected Balb/3T3 cells. Each panel (**A**–**C**) was labeled accordingly: non-transfected cells (control, **lane 1**) or transfected with the empty pEGFP-N3 vector (**lane 2**) or the fusion constructs EGFP-AnxA6-1 (**lane 3**) and EGFP-AnxA6-2 (**lane 4**). All samples (10^6 cells) were washed, stained by PI and analyzed directly by flow cytometer to determine cell viability (**A**), cell size (**B**), and cell granularity (**C**). The mean of three separate experiments, each performed in duplicate, is shown.

conditions 66% of endogenous AnxA6 remained membrane-attached (Table III). Addition of 2 mM $CaCl_2$ resulted in the isolation of AnxA6-1 and AnxA6-2 predominantly in the membrane-bound pool along with 100% of endogenous AnxA6.

Intracellular distribution of AnxA6 isoforms may be related to their functions in endocytosis. Indeed, experimental evidence indicated a potential role of AnxA6 at late stages of endocytosis [Grewal et al., 2000]. Therefore, we employed the method of cellular fractionation by centrifugation in sucrose density gradients designed to separate early and late endosomal fractions from heavy membranes (e.g., the plasma membrane, Golgi apparatus, and endoplasmic reticulum) and analyzed for the presence of AnxA6 and marker proteins characteristic for each particular cellular compartment. To examine the possible involvement of AnxA6 isoforms in endocytosis, we modulated this process by incubating the cells at different Ca^{2+} and H^+ extracellular concentrations.

Table IV shows the distribution of endogenous AnxA6 and AnxA6 isoforms in interphases collected from sucrose gradient (8–40%, w/v). In the presence of 5 mM EGTA at pH 7.4, endogenous AnxA6 was detected in the form attached to both types of endosomal membranes, LE and EE (interphases 1 and 2). Under the same conditions, AnxA6-1 was found mostly associated with EE (interphase 2) whereas AnxA6-2, similarly to endogenous AnxA6, accumulated at endosomal membranes (interphases 1 and 2). Extracellularly added 1 mM $CaCl_2$ at pH 6.0 induced partial relocation of endogenous AnxA6 from endosomes to HM (interphase 3). In this experimental variant, AnxA6-1 relocated from EE to LE and HM (interphase 1 and 3, respectively). A significant pool of AnxA6-2 was identified attached to EE (interphase 2).

To confirm these observations, we compared the distribution of AnxA6 and isoforms with AnxA2 and markers of EE (Rab5B) [Gorvel et al., 1991], LE (Rab7) [Chavrier et al., 1990], and the plasma membrane (SNAP-25) [McMahon and Sudhof, 1995] in non-transfected cells as control cells. In 5 mM EGTA at pH 7.4, AnxA2 and Rab5B were detected mainly in EE whereas Rab7 was identified only in LE. Incubation of cells in the presence of 1 mM $CaCl_2$ at pH 6.0 induced relocation of endogenous AnxA2 to HM identified by the presence of SNAP-25, whereas marker proteins of endocytosis persisted mainly in early (Rab5B) or late (Rab7) endosomal fractions (data not shown). Some accumulation of Rab5B and Rab7 was also observed in HM suggesting attachment of transport vesicles with the plasma membrane upon increase of $[Ca^{2+}]_{in}$.

Immunocytochemical experiments performed under the same stimulatory conditions showed co-localization of endogenous AnxA6 with plasma membrane marker, SNAP-25 (Fig. 10G, arrows) and with vesicular membranes stained by EE marker Rab5B (Fig. 10A, arrows) and

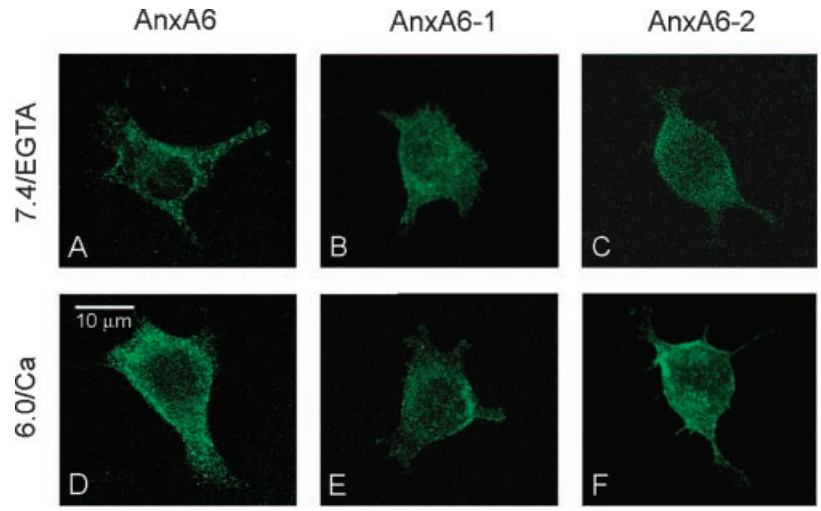

Fig. 8. A Ca^{2+} and H^+-dependent relocation of endo- and exogenous AnxA6 isoforms in Balb/3T3 cells. Non-transfected Balb/3T3 cells (**A**,**D**) and transfected with fusion constructs EGFP-AnxA6-1 (**B**,**E**) or EGFP-AnxA6-2 (**C**,**F**) are presented. Cells were incubated 10 min/20°C in different extracellular Ca^{2+} and H^+ concentrations in the PD buffer: pH 7.4/5 mM EGTA (**A**–**C**) or pH 6.0/1 mM $CaCl_2$ (**C**,**D**,**F**). After fixation and permeabilization, the subcellular relocation of endogenous AnxA6 (**A**,**D**) was detected by mouse anti-AnxA6 antibody followed by anti-mouse-IgG FITC staining and confocal laser scan microscopy but relocation of EGFP-AnxA6 isoforms (**B**,**C**,**E**,**F**) was detected directly by confocal laser scan microscopy.

LE marker Rab7 (Fig. 10D, arrows). We also observed that stimulation promoted association of AnxA6 isoforms with plasma membrane as confirmed by co-localization of both isoforms with the plasma membrane marker SNAP-25 (Fig. 10H,I, arrows). Furthermore, vesicular membranes were identified as endosomes since AnxA6-1 co-localized with EE marker Rab5B (Fig. 10B, arrows) and with LE marker Rab7 (Fig. 10E, arrows), while AnxA6-2 co-localized only with EE marker Rab5B (Fig. 10C, arrows).

DISCUSSION

Properties of Recombinant AnxA6 Isoforms

Up to now, most accumulated information about AnxA6 is in fact related to isoform AnxA6-1, since it is well known that in mammalian cells AnxA6-1 predominates. The only known exception is tumor cells where the expression levels of AnxA6-1 and AnxA6-2 are of the same range [Edwards and Moss, 1995]; however, a larger number of cancer cell lines and tissues should be

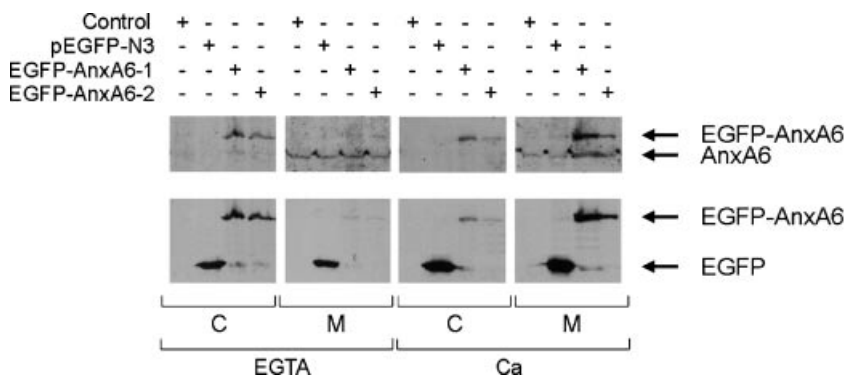

Fig. 9. Distribution of endo- and exogenous AnxA6 isoforms in Balb/3T3 cells. Immunoblots of whole cell homogenates were prepared from 10^8 non-transfected (control) and cells transfected with the empty pEGFP-N3 vector or the fusion constructs EGFP-AnxA6-1 and EGFP-AnxA6-2. Cells were extracted 30 min/4°C in TLB supplemented with 2 mM $CaCl_2$ or 5 mM EGTA and disrupted by repeated sonication cycles. After centrifugation, supernatants as cytosolic fraction (C) were collected, pellets as membrane fraction (M) were dissolved in TLB containing 20 mM EGTA and the solubilization process was repeated. Proteins were separated on 10% SDS–PAGE and transferred to nitrocellulose membranes. Probes were incubated with mouse anti-AnxA6 antibody (**upper panel**) or were stained with an antibody to GFP (**lower panel**). The positions of endogenous AnxA6, EGFP, and EGFP-AnxA6 isoform constructs are indicated. One typical experiment out of five is shown.

TABLE III. Quantitative Analysis of AnxA6 Distribution in Cytosolic and Membrane Fraction of Transfected Mouse Balb/3T3 Fibroblasts

	+ EGTA		+ Ca^{2+}	
Protein	Cytosolic fraction	Membrane fraction	Cytosolic fraction	Membrane fraction
Endogenous AnxA6	33.9	66.1	0.2	99.8
Exogenous AnxA6-1	77.0	23.0	25.0	75.0
Exogenous AnxA6-2	87.4	12.6	36.0	64.0

The amount of protein in cytosolic and membrane fractions, expressed as % of total protein present in both fractions, was determined by densitometric analysis of the Western blot shown in Figure 9.

analyzed to draw a confident conclusion. The first evidence that AnxA6 isoforms may have different functions came from the observation that A431 cells expressing AnxA6-1 are defective in their ability to sustain elevated levels of cytosolic Ca^{2+} and exhibit changes in cellular phenotype and growth rate [Fleet et al., 1999]. It can be hypothesized that changes in expression of AnxA6 isoforms may affect signal transduction in tumor cells which lead to multidrug resistance [Liscovitch and Lavie, 2000]. In other systems, it was reported that changes in expression of AnxA6 may result in hypertrophy of cardiac muscle and stroke [Hawkins et al., 1999].

In this report we characterized differences between AnxA6 isoforms in molecular shape and in their sensitivity to [Ca^{2+}] and to [H^{+}]. The lack of six amino acid residues in AnxA6-2 affected the mechanism of binding of this isoform to membranes and its affinity to cations as well as its intracellular targeting. The latter is corroborated by the behavior of the VAAEIL containing Rab28. In this case, alternative mRNA splicing generates two isoforms, Rab28S and Rab28L, characterized by different C-termini close to the VAAEIL sequence [Brauers et al., 1996]. As a probable consequence, Rab28S is detected in most investigated tissues whereas Rab28L predominates in testis. Per analogy, we propose that the lack of the VAAEIL sequence in AnxA6-2 and distinct properties of this isoform in comparison to AnxA6-1 could influence the localization of AnxA6-1 and AnxA6-2 to specific cellular compartments where they elicit different regulatory functions. In this report we demonstrated that AnxA6 isoforms differ in their extractability with non-ionic detergent, permitting the visualization of two distinct populations of AnxA6. This is consistent with the earlier reported ability of annexins to attach to the plasma membrane [Clemen et al., 1999; McNeil et al., 2006; Chang et al., 2007] or to interact with the actin cytoskeleton [Lauvrak et al., 2005; Hayes et al., 2006]. In addition, one should consider that PM and endosomal compartments consist of multiple membrane domains with different solubility (raft and non-raft regions) and different mode of interaction with the actin cytoskeleton [Hayes et al., 2004; Babiychuk and Draeger, 2006; Falsey et al., 2006; Goebeler et al., 2006].

TABLE IV. Subcellular Distribution of Endo- and Exogenous AnxA6 Isoforms in Balb/3T3 Cells

	7.4/EGTA			6.0/Ca		
	LE	EE	HM	LE	EE	HM
Endogenous AnxA6	23.0 ± 2.3	22.0 ± 2.1	2.4 ± 0.3	17.2 ± 1.6	6.6 ± 0.6	15.5 ± 1.6
Exogenous AnxA6-1	5.4 ± 0.5	61.8 ± 5.8	14.3 ± 1.3	21.0 ± 2.0	10.7 ± 0.9	34.4 ± 3.2
Exogenous AnxA6-2	34.0 ± 3.0	29.2 ± 3.0	4.6 ± 0.6	1.4 ± 0.2	64.8 ± 6.5	0.9 ± 0.1

EE and LE were separated from HM by sucrose gradient cell fractionation. Non-transfected cells and cells transfected with the fusion constructs pEGFP-AnxA6-1 or pEGFP-AnxA6-2 (1.5×10^8 of cells per each experimental variant) were incubated under different conditions: control (in the presence of 5 mM EGTA at pH 7.4) or stimulated (in the presence of 1 mM $CaCl_2$ at pH 6.0). After stimulation cells were homogenized and centrifuged 1,200*g*/15 min/4°C. PNS was loaded at the bottom of the sucrose gradient and centrifuged at 220,000*g*/120 min/4°C. In three interphases (LE, EE, and HM), the presence of endogenous AnxA6, and exogenous AnxA6-1 and AnxA6-2 was tested by Western blotting. The relative intensities of the labeled bands were measured densitometrically. Data are the mean of protein content (in % of total protein found in a gradient including interphases and other fractions) for three experiments.

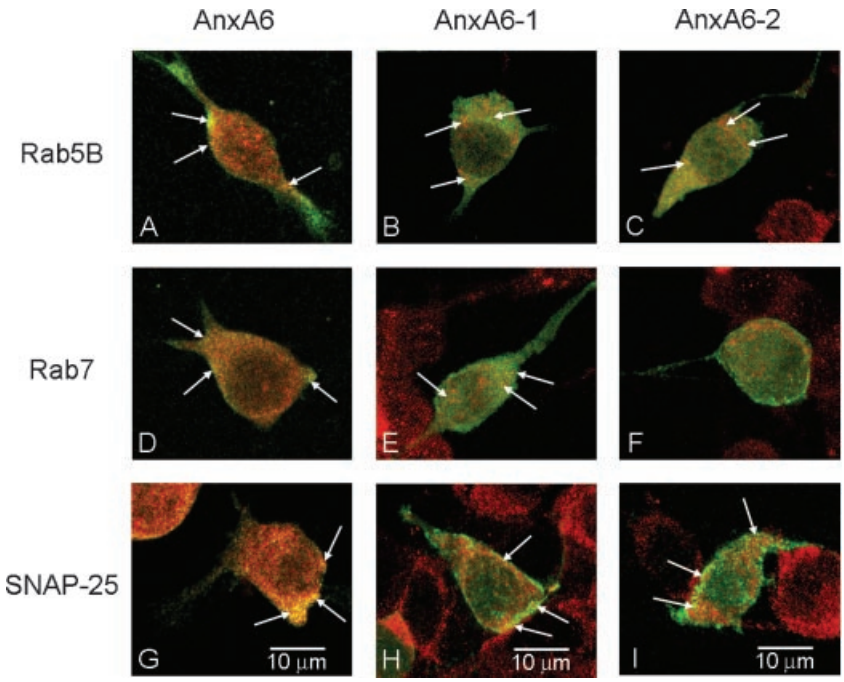

Fig. 10. The effect of Ca^{2+} or H^+ on co-localization of endo- and exogenous AnxA6 isoforms with endocytic pathway markers in Balb/3T3 cells. Non-transfected Balb/3T3 cells (**A**,**D**,**G**) and transfected with EGFP-AnxA6-1 (**B**,**E**,**H**) or EGFP-AnxA6-2 (**C**,**F**,**I**) fusion constructs are presented. Cells were incubated 10 min/20°C in extracellular Ca^{2+} (1 mM $CaCl_2$) and H^+ (pH 6.0) concentrations in PD buffer. After fixation and permeabilization, the subcellular localizations of AnxA6-1 and AnxA6-2 isoforms were detected directly by confocal laser scan microscopy. The co-localizations of endogenous AnxA6 with Rab5B (**A**–**C**), Rab7 (**D**–**F**), and SNAP-25 (**G**–**I**) were detected by anti-mouse-FITC with anti-mouse rhodamine or anti-rabbit-TRITC staining, respectively. Protein co-localizations are indicated in yellow and with arrows in merge panels.

AnxA6-Isoform Transfected Balb/3T3 Fibroblasts

Our findings using Balb/3T3 fibroblasts upon transfection with cDNAs encoding either AnxA6 isoform demonstrated distinct cellular localization of newly expressed AnxA6-1 and AnxA6-2. Moreover, AnxA6 isoforms differently responded to moderate changes in $[Ca^{2+}]_{in}$ and $[H^+]_{in}$, consistent with their different abilities in vitro to respond to changes in $[Ca^{2+}]$ and/or in $[H^+]$. This may suggest that intracellular localization and functions of AnxA6 isoforms are differently regulated during vesicular traffic. Concerning other isoforms within the annexin family of proteins, isoforms of AnxA7 and AnxA13 have 22 or 41 extra codons encoded by cassette exons 6 or 2, respectively [Lecat et al., 2000; Herr et al., 2003]. AnxA13 is distributed in epithelial cells in two forms associated with apical and basolateral membranes. However, only the basolateral form of AnxA13 requires calcium for association with plasma membrane microdomains, rafts. AnxA13b isoform is attached exclusively to the apical membrane where it is involved in raft-mediated delivery of proteins [Lecat et al., 2000].

The intracellular distribution of AnxA6 isoforms between cytosol and membrane fraction changed with the increase of $[Ca^{2+}]$. Our findings are similar to data showing membrane association of AnxA7 isoforms mediated by Ca^{2+} [Clemen et al., 1999; Herr et al., 2003], but in contrast to AnxA7 isoforms, AnxA6-1 can only be released from membrane by extraction in the presence of high EGTA concentrations, suggesting calcium-independent binding. Similar Ca^{2+}-independent membrane binding was also reported for AnxA2 for which nearly 50% of the total annexin pool was tightly associated with membranes [Harder et al., 1997; Jost et al., 1997]. AnxA13b exhibits detergent-resistant membrane association, being a component of membrane fraction representing microdomains enriched with cholesterol and glycosphingolipids [Lafont et al., 1998].

Changes in $[Ca^{2+}]_{in}$ and $[H^+]_{in}$ seem to be key factors affecting subcellular distribution of AnxA6 isoforms. However, participation of accessory proteins cannot be neglected. Some

experimental evidence suggests that AnxA6 relocation from cytoplasm to membranes is related to interaction with actin filaments and/or small GTPase [Macia et al., 2004; Venkateswarlu et al., 2004] and is corroborated by earlier reports showing that AnxA6 binds actin filaments in a Ca^{2+}- and lipid-dependent manner [Hosoya et al., 1992; Watanabe et al., 1994]. As another example, in smooth muscle cells it was proposed that binding of actin monomers at the pointed end of actin filament and Ca^{2+}-dependent association with lipid rafts mediate the relocation of AnxA6 from cytosol to plasma membrane microdomains [Babiychuk et al., 1999; Babiychuk and Draeger, 2000]. In addition, our experimental data suggest a new pH-dependent mechanism that regulates cytoskeleton- and membrane-binding of AnxA6. For most of the AnxA6-2 pool the presence of Ca^{2+} was not necessary for F-actin binding. Furthermore, in agreement with conclusions made by Kaetzel et al. [1994], AnxA6-2 was less hydrophobic in the presence of EGTA and the key for successful aqueous/detergent phase separation in the presence of Triton X-114 was the lowering of pH to 4.0, as described earlier for tissue purified and recombinant AnxA6-1 isoform [Golczak et al., 2001a; Kirilenko et al., 2002].

We suggest that AnxA6 isoforms may be key players in the pathway regulating endocytic membrane fusion and degradation [Simonsen et al., 1998]. Analysis by fractionation in sucrose gradients of subcellular distribution of AnxA6 isoforms in endocytotic compartments revealed for the first time that in resting cells, AnxA6-1 is associated with EE, and AnxA6-2 with LE. A moderate increase in $[Ca^{2+}]_{in}$ and/or $[H^+]_{in}$ induced relocation of AnxA6-1 to LE and HM but AnxA6-2 to EE. Our findings are in agreement with those obtained by other investigators who found AnxA6 mainly in cytosol, endosomal compartment and on plasma membrane in CHOwt and CHOanx6 cells [Grewal et al., 2000; de Diego et al., 2002]. Moreover, by showing membrane binding of AnxA6 isoforms in the presence of EGTA, we confirmed earlier observations identifying two pools of AnxA6 molecules, Ca^{2+}-dependent and Ca^{2+}-independent, associated either with EE or LE, respectively [de Diego et al., 2002]. The novelty of the present observation is the dissection of intracellular localization of both isoforms and that it shows their independent relocation upon cell stimulation.

In conclusion, we propose that the discrete structural and functional differences between AnxA6 isoforms promoting distinct localization of these isoforms to specific cellular compartments is probably a molecular mechanism of participation of AnxA6 isoforms in Ca^{2+}- and H^+-dependent membrane dynamics during vesicular transport.

ACKNOWLEDGMENTS

We would like to thank Drs. Yogesh C. Awasthi, Marie-France Bader, Volker Gerke, Patrick Groves, and Stephen E. Moss for critical reading of the manuscript. We thank Dr. John Carew for correcting the English.

REFERENCES

Babiychuk EB, Draeger A. 2000. Annexins in cell membrane dynamics. Ca^{2+}-regulated association of lipid microdomains. J Cell Biol 150:1113–1124.

Babiychuk EB, Draeger A. 2006. Biochemical characterization of detergent-resistant membranes: A specific approach. Biochem J 397:407–416.

Babiychuk EB, Palstra RJ, Schaller J, Kampfer U, Draeger A. 1999. Annexin VI participates in the formation of a reversible, membrane-cytoskeleton complex in smooth muscle cells. J Biol Chem 274:35191–35195.

Bandorowicz J, Pikula S, Sobota A. 1992. Annexins IV (p32) and VI (p68) interact with erythrocyte membrane in a calcium-dependent manner. Biochim Biophys Acta 1105: 201–206.

Benz J, Bergner A, Hofmann A, Demange P, Gottig P, Liemann S, Huber R, Voges D. 1996. The structure of recombinant human annexin VI in crystals and membrane-bound. J Mol Biol 260:638–643.

Bordier C. 1981. Phase separation of integral membrane proteins in Triton X-114 solution. J Biol Chem 256:1604–1607.

Bradford MM. 1976. A rapid and sensitive method for the quantitation of microgram quantities of protein utilizing the principle of protein-dye binding. Anal Biochem 7: 248–254.

Brauers A, Schurmann A, Massmann S, Mul-Zurbes P, Becker W, Kainulainen H, Chichung L, Joost H-G. 1996. Alternative mRNA splicing of the novel GTPase Rab28 generates isoforms with different C-termini. Eur J Biochem 237:833–840.

Burger A, Berendes R, Voges D, Huber R, Demange P. 1993. A rapid and efficient purification method for recombinant annexin V for biophysical studies. FEBS Lett 329:25–28.

Chang N, Sutherland C, Hesse E, Winkfein R, Wiehler WB, Pho M, Veillette C, Li S, Wilson DP, Kiss E, Walsh MP. 2007. Identification of a novel interaction between the Ca^{2+}-binding protein S100A11 and the Ca^{2+}- and phospholipid-binding protein annexin A6. Am J Physiol Cell Physiol 292:C1417–C1430.

Chavrier P, Parton RG, Hauri HP, Simons K, Zerial M. 1990. Localization of low molecular weight GTP binding

proteins to exocytic and endocytic compartments. Cell 62:317–329.

Chow A, Gawler D. 1999. Mapping the site of interaction between annexin VI and the $p120^{GAP}$ C2 domain. FEBS Lett 460:166–172.

Clemen CS, Hofmann A, Zamparelli C, Noegel AA. 1999. Expression and localization of annexin VII (synexin) isoforms in differentiating myoblasts. J Muscle Res Cell Motil 20:669–679.

Davies AA, Moss SE, Crumpton MR, Jones TA, Spurr NK, Sheer D, Kozak C, Crumpton MJ. 1989. The gene coding for the p68 calcium-binding protein is localized to bands q32-q34 of human chromosome 5, and to mouse chromosome 11. Hum Genet 82:234–238.

Davis AJ, Butt JT, Walker JH, Moss SE, Gawler DJ. 1996. The Ca^{2+}-dependent lipid binding domain of $P120^{GAP}$ mediates protein–protein interactions with Ca^{2+}-dependent membrane-binding proteins. Evidence for a direct interaction between annexin VI and $P120^{GAP}$. J Biol Chem 271:24333–24336.

de Diego I, Schwartz F, Siegfried H, Dauterstedt P, Heeren J, Beisiegel U, Enrich C, Grewal T. 2002. Cholesterol modulates the membrane binding and intracellular distribution of annexin 6. J Biol Chem 277:32187–32194.

Dominik M, Klopocka W, Pomorski P, Kocik E, Redowicz JM. 2005. Characterization of Amoeba proteus myosin VI immunoanalog. Cell Motil Cytoskeleton 61:172–188.

Draeger A, Wray S, Babiychuk EB. 2005. Domain architecture of the smooth-muscle plasma membrane: Regulation by annexins. Biochem J 387:309–314.

Dressler LG. 1988. DNA flow cytometry and prognostic factors in 1331 frozen breast cancer speciments. Cancer 61:420–427.

Dubois T, Soula M, Moss SE, Russo-Marie F, Rothhut B. 1995. Potential interaction between annexin VI and a 56-kDa protein kinase in T cells. Biochem Biophys Res Commun 212:270–278.

Edwards HC, Moss SE. 1995. Functional and genetic analysis of annexin VI. Mol Cell Biochem 149/150:293–299.

Falsey RR, Marron MT, Gunaherath GM, Shirahatti N, Mahadevan D, Gunatilaka AA, Whitesell L. 2006. Actin microfilament aggregation induced by withaferin A is mediated by annexin II. Nat Chem Biol 2:33–38.

Filipenko NR, Waisman DM. 2001. The C terminus of annexin II mediates binding to F-actin. J Biol Chem 276: 5310–5315.

Fleet A, Ashworth R, Kubista H, Edwards H, Bolsover S, Mobbs P, Moss SE. 1999. Inhibition of EGF-dependent calcium influx by annexin VI is splice form-specific. Biochem Biophys Res Commun 260:540–546.

Freye-Minks C, Kretsinger RH, Creutz CE. 2003. Structural and dynamic changes in human annexin VI induced by a phosphorylation-mimicking mutation, T356D. Biochemistry 42:620–630.

Gerke V, Moss SE. 2002. Annexins: From structure to function. Physiol Rev 82:331–371.

Gerke V, Creutz CE, Moss SE. 2005. Annexins: Linking Ca^{2+} signalling to membrane dynamics. Nat Rev Mol Cell Biol 6:449–461.

Goebeler V, Ruhe D, Gerke V, Resher U. 2006. Annexin A8 displays unique phospholipid and F-actin binding properties. FEBS Lett 580:2430–2434.

Golczak M, Kicinska A, Bandorowicz–Pikula J, Buchet R, Szewczyk A, Pikula S. 2001a. Acidic pH-induced folding of annexin VI is a prerequisite for its insertion into lipid bilayers and formation of ion channels by the protein molecule. FASEB J 15:1083–1085.

Golczak M, Kirilenko A, Bandorowicz-Pikula J, Pikula S. 2001b. Conformational states of annexin VI in solution induced by acidic pH. FEBS Lett 496:49–54.

Gorvel JP, Chavrier P, Zerial M, Gruenberg J. 1991. Rab5 controls early endosome fusion in vitro. Cell 64:915–925.

Grewal T, Heeren J, Mewawala D, Schnitgerhans T, Wendt D, Salomon G, Enrich C, Beisiegel U, Jäckle S. 2000. Annexin VI stimulates endocytosis and is involved in the trafficking of low density lipoprotein to the prelysosomal compartment. J Biol Chem 275:33806–33813.

Grewal T, Evans R, Rentero C, Tebar F, Cubells L, de Diego I, Kirchhoff MF, Hughes WE, Heeren J, Rye K-A, Rinninger F, Daly RJ, Pol A, Enrich C. 2005. Annexin A6 stimulates the membrane recruitment of $p120^{GAP}$ to modulate Ras and Raf-1 activity. Oncogene 24:5809–5820.

Harder T, Kelner R, Parton RG, Gruenberg J. 1997. Specific release of membrane-bound annexin II and cortical cytoskeletal elements by sequestration of membrane cholesterol. Mol Biol Cell 8:533–545.

Hawkins TE, Roes D, Monkhouse J, Moss SE. 1999. Immunological development and cardiovascular function are normal in annexin VI null mutant mice. Mol Cell Biol 19:8028–8032.

Hayes MJ, Resher U, Gerke V, Moss SE. 2004. Annexin–actin interactions. Traffic 5:571–576.

Hayes MJ, Shao D, Bailly M, Moss SE. 2006. Regulation of actin dynamics by annexin 2. EMBO J 25:1816–1826.

Herr C, Clemen CS, Lehnert G, Kutschkow R, Picker SM, Gathof BS, Zamparelli C, Schleicher M, Noegel AA. 2003. Function, expression and localization of annexin A7 in platelets and red blood cells: Insights derived from an annexin A7 mutant mouse. BMC Biochem 4:8.

Hooper NM. 1992. Identification of a glycosylphophatidylinositol anchor on membrane proteins. In: Hooper NM, Tuner AJ, editors. Lipid modifications of proteins: A practical approach. Leeds: IRL Press. pp 89–113.

Hosoya H, Kobayashi R, Tsukita S, Matsumura F. 1992. Ca^{2+}-regulated actin and phospholipids binding protein (68 kD-protein) from bovine liver: Identification as a homologue for annexin VI and intracellular localization. Cell Motil Cytoskeleton 22:200–210.

Huang JW, Chen CL, Chuang NN. 2005. P120-GAP associated with syndecan-2 to function as an active switch signal for Src upon transformation with oncogenic Ras. Biochem Biophys Res Commun 329:855–862.

Jost M, Zeuschner D, Seemann J, Weber K, Gerke V. 1997. Identification and characterization of a novel type of annexin-membrane interaction: Ca^{2+} is not required for the association of annexin II with early endosomes. J Cell Sci 110:221–228.

Kaetzel MA, Pula G, Campos B, Uhrin P, Horseman N, Dedman JR. 1994. Annexin VI isoforms are differentially expressed in mammalian tissues. Biochim Biophys Acta 1223:368–374.

Kamal A, Ying Y, Anderson RG. 1998. Annexin VI-mediated loss of spectrin during coated pit budding is coupled to delivery of LDL to lysosomes. J Cell Biol 142: 937–947.

Kim GG, Donnenberg VS, Donnenberg AD, Gooding W, Whiteside TL. 2007. A novel multiparametric flow cytometry-based cytotoxicity assay simultaneously immunophenotypes effector cells: Comparisons to a 4 h (51)Cr-release assay. J Immunol Methods 325:51–66.

Kirilenko A, Golczak M, Pikula S, Buchet R, Bandorowicz-Pikula J. 2002. GTP-induced membrane binding and ion channel activity of annexin VI: Is annexin VI a GTP biosensor? Biophys J 82:2737–2745.

Kirilenko A, Pikula S, Bandorowicz-Pikula J. 2006. Effects of mutagenesis of W343 in human annexin A6 isoform 1 on its interaction with GTP: Nucleotide-induced oligomer formation and ion channel activity. Biochemistry 45: 4965–4973.

Krishan A. 1975. Rapid flow cytometric analysis of mammalian cell cycle by propidium iodide staining. J Cell Biol 66:188–193.

Lafont F, Lecat S, Verkade P, Simons K. 1998. Annexin XIIIb associates with lipid microdomains to function in apical delivery. J Cell Biol 142:1413–1427.

Lauvrak SU, Hollas H, Doskeland AP, Aukrust I, Flatmark T, Vedeler A. 2005. Ubiquitinated annexin A2 is enriched in the cytoskeleton fraction. FEBS Lett 579:203–206.

Lecat S, Verkade P, Thiele C, Fiedler K, Simons K, Lafont F. 2000. Different properties of two isoforms of annexin XIII in MDCK cells. J Cell Sci 113:2607–2618.

Lin HC, Sudhof TC, Anderson RG. 1992. Annexin VI is required for budding of clathrin-coated pits. Cell 70:283–291.

Liscovitch M, Lavie Y. 2000. Multidrug resistance: A role for cholesterol efflux pathways? Trends Biochem Sci 25:530–534.

Macia E, Luton F, Partisani M, Cherfils J, Chardin P, Franco M. 2004. The GDP-bound form of Arf6 is located at the plasma membrane. J Cell Sci 117:2389–2398.

McMahon HT, Sudhof TC. 1995. Synaptic core complex of synaptobrevin, syntaxin, and SNAP-25 forms high affinity α-SNAP binding site. J Biol Chem 270:2213–2217.

McNeil AK, Rescher U, Gerke V, McNeil PL. 2006. Requirement for annexin A1 in plasma membrane repair. J Biol Chem 281:35202–35207.

Montaville P, Neumann JM, Russo-Marie F, Ochsenbein F, Sanson A. 2002. A new consensus sequence for phosphatidylserine recognition by annexins. J Biol Chem 277: 24684–24693.

Naslavsky N, Weigert R, Donaldson JG. 2003. Convergence of non-clathrin- and clathrin-derived endosomes involves Arf6 inactivation and changes in phosphoinositides. Mol Biol Cell 14:417–431.

Pons M, Tebar F, Kirchhoff M, Peiro S, de Diego I, Grewal T, Enrich C. 2001. Activation of Raf-1 is defective in annexin 6 overexpressing Chinese hamster ovary cells. FEBS Lett 501:69–73.

Reeves JP, Dowben RM. 1969. Formation and properties of thin-walled phospholipid vesicles. J Cell Physiol 73: 49–60.

Rescher U, Gerke V. 2004. Annexins—unique membrane binding proteins with diverse functions. J Cell Sci 117: 2631–2639.

Rescher U, Ruche D, Ludwig C, Zobiack N, Gerke V. 2004. Annexin 2 is a phosphatidylinositol (4,5)-bisphosphate binding protein recruited to actin assembly sites at cellular membranes. J Cell Sci 117:3473–3480.

Rodbard D, Chrambach A. 1971. Estimation of molecular radius, free mobility, and valence using polyacrylamide gel electrophoresis. Anal Biochem 40:95–134.

Schmitz-Peiffer C, Browne CL, Walker JH, Biden TJ. 1998. Activated protein kinase C alpha associates with annexin VI from skeletal muscle. Biochem J 330:675–681.

Simonsen A, Lippe R, Christofordis S, Gaullier J-M, Brech A, Callaghan J, Toh B-H, Murphy C, Zerial M, Stenmark H. 1998. EEA1 links PI(3)K function to Rab 5 regulation of endosome fusion. Nature 394:494–498.

Smythe E, Smith PD, Jacob SM, Theobald J, Moss SE. 1994. Endocytosis occurs independently of annexin VI in human A431 cells. J Cell Biol 24:301–306.

Song G, Harding SE, Duchen MR, Tunwell R, O'Gara P, Hawkins TE, Moss SE. 2002. Altered mechanical properties and intracellular calcium signaling in cardiomyocytes from annexin 6 null-mutant mice. FASEB J 16: 622–624.

Strzelecka A, Pyrzynska B, Kwiatkowska K, Sobota A. 1997. Syk kinase, tyrosine-phosphorylated proteins and actin filaments accumulate at forming phagosomes during Fcγ receptor-mediated phagocytosis. Cell Motil Cytoskel 38:287–296.

Strzelecka-Kiliszek A, Kwiatkowska K, Sobota A. 2002. Lyn and Syk kinases are sequentially engaged in phagocytosis mediated by Fc gamma R. J Immunol 169: 6787–6794.

Venkateswarlu K, Brandom KG, Lawrence JL. 2004. Centaurin-alpha1 is an in vivo phosphatidylinositol 3,4,5-trisphosphate-dependent GTPase-activating protein for ARF6 that is involved in actin cytoskeleton organization. J Biol Chem 279:6205–6208.

Watanabe T, Inui M, Chen BY, Iga M, Sobue K. 1994. Annexin VI-binding proteins in brain. Interaction of annexin VI with a membrane skeletal protein, calspectin (brain spectrin or fodrin). J Biol Chem 69:17656–17662.

Wei X, Henke VG, Strubin C, Brown EB, Clapham DE. 2003. Real-time imaging of nuclear permeation by EGFP in single intact cells. Biophys J 84:1317–1327.

Zablocki K, Makowska A, Duszynski J. 2003. pH-dependent effect of mitochondria on calcium influx into Jurkat cells; a novel mechanism of cell protection against calcium entry during energy stress. Cell Calcium 33: 91–99.